Simulation and Design of a Heterogeneously Integrated III-V/Silicon Dual-wavelength Laser

Yingchen Wu and Jian-Jun He
State Key Laboratory of Modern Optical Instrumentation, Centre for Integrated Optoelectronics
Department of Optical Engineering, Zhejiang University, Hangzhou 310027, China

Abstract— We present the design and simulation results of a novel dual-wavelength laser based on III-V/silicon heterogeneously integration platform. A single-mode symmetric splitting in reflection spectrum appears when embedding shoulder gratings inside a micro-ring resonator. We use the grating micro-ring (GMR) as the front reflector of the laser. By adjusting the reflection coefficient of the gratings and the coupling coefficient between the ring and the straight waveguide, the difference between the two lasing wavelengths can vary from 0 to more than 1 nm.

1. INTRODUCTION

Terahertz wireless communication is considered as an excellent candidate to meet the rapidly increasing demand for broadband wireless network, due to its inherently higher bandwidth compared to microwave solutions [1]. Mode-beating dual-wavelength lasers, which can be used for continuous wave (CW) THz carrier signal generation [2] and all-optical clock recovery [3], have attracted significant attention. Monolithically integrated dual-wavelength lasers (DWLs) are more compact, cost-effective than the free-running laser pair [4] as an optical beat source. Compared to two discrete free-running lasers, the DWL has more stable frequency leading to a smaller drift of the THz signal when undergoing similar environmental fluctuations. Several ways to achieve monolithically integrated dual wavelength laser have been published, such as multi-section distributed feedback (DFB) lasers [5, 6], independent lasers on a chip with optical combiner [7] and single cavity dual-wavelength laser [8, 9].

In this paper, we demonstrate a novel hybrid integrated DWL. By incorporating a shoulder grating into a micro-ring, we can enhance the coupling between the two counter-propagating modes. The reflection spectrum of GMR shows symmetric splitting when the reflection coefficient of the gratings and the coupling coefficient between the ring and the straight waveguide are appropriately designed.

2. DEVICE PRINCIPLE

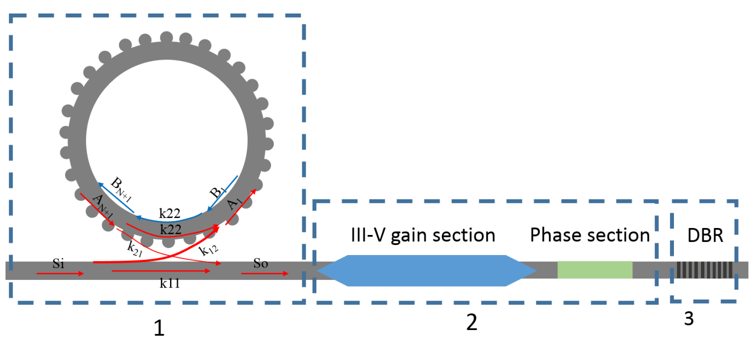

Figure 1: The schematic of the dual-wavelength laser.

The structure of the DWL is shown in Fig. 1. It can be divided into 3 sections: Section 1 for the grating embedded micro-ring, Section 2 for the gain and phase adjustment, and Section 3 for the DBR as rear reflector.

The DWL can be monolithically integrated by BCB bonding technique on SOI wafer [10]. The shoulder gratings are embedded into the entire micro-ring resonator. The regular period of the shoulder gratings is equal to half of the angular period of the micro-ring resonance order, so it couples with only one resonance mode [11].

We use the transfer matrix method for simulation. For the ring part, as shown in Fig. 1, k_{11} and k_{22} are self-coupling coefficients, we have $k_{11}^* = k_{22}$, k_{12} and k_{21} are cross-coupling coefficients, and we have $k_{12}^* = -k_{21}$, $k_{11}k_{12} - k_{21}k_{12} = 1$, n stands for the number of periods of the grating. The transmission matrix of the ring is given by.

$$\left[\begin{array}{c} S_i \\ S_0 \end{array}\right] = \frac{1}{k_{12}} \left[\begin{array}{cc} 1 & -k_{11}^* \\ k_{11} & -1 \end{array}\right] \left[\begin{array}{c} A_1 \\ A_{n+1} \end{array}\right] \tag{1}$$

Representing the relation between A_{n+1} and A_1 by $A_{n+1} = f(A_1)$, we can obtain

$$S_i = \frac{A_1 - k_{11}^* f(A_1)}{k_{12}}, S_o = \frac{k_{11}A_1 - f(A_1)}{K_{12}} \tag{2}$$

Considering the grating, as shown in Fig. 2, we use the transmission matrix T for the interface of two medium and P for homogeneous medium. Λ is the period of grating, L_1 is the length of grating teeth, D (defined as L_1/Λ) is the duty cycle of the grating, r is the reflection coefficient at interface, A_i (or B_i) gives steady-state amplitudes of the forward (or backward) mode at different periods.

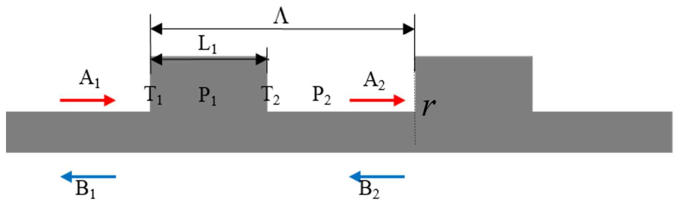

Figure 2: Schematic of the gratings.

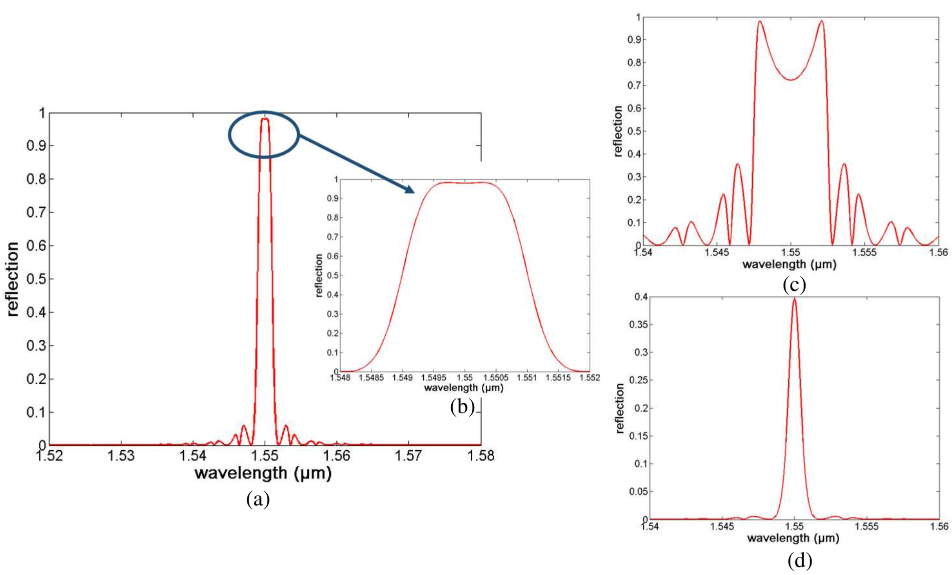

Figure 3: (a) The reflection spectrum of GMR when $r = 0.001$, $k_{11} = 0.3$. (b) Enlarged view of the spectrum around reflection peak. (c) Reflection spectrum when $r = 0.002$, $k_{11} = 0.3$. (d) Reflection spectrum when $r = 0.0003$, $k_{11} = 0.3$.

The relations between $A_1, B_1, A_{n+1}, B_{n+1}$ can therefore be written as follows:

$$\left[\begin{array}{c} A_1 \\ B_1 \end{array}\right] = [T_1P_1T_2P_2]^n \left[\begin{array}{c} A_{n+1} \\ B_{n+1} \end{array}\right] = M \left[\begin{array}{c} A_{n+1} \\ B_{n+1} \end{array}\right]. \tag{3}$$

Use Bloch wave method to solve the M matrix:

$$M = \left[\begin{array}{cc} m_{11}U_{N-1} - U_{N-2} & m_{12}U_{N-1} \\ m_{21}U_{N-1} & m_{22}U_{N-1} - U_{N-2} \end{array}\right], \tag{4}$$

where

$$U_N = \frac{\sin\left(\left(N+1\right)K\Lambda\right)}{\sin\left(K\Lambda\right)}, K\Lambda = \cos^{-1}\left(\frac{m_{11}+m_{22}}{2}\right). \tag{5}$$

The relation between B_1 and B_{n+1} is as follows:

$$B_{n+1} = k_{22}B_1 = k_{11}B_1 \tag{6}$$

From Equations (2)–(6), we can obtain:

$$\frac{S_o}{S_i} = \frac{k_{11}M_{11} + k_{11}^{*}M_{22} - k_{11}k_{11}^{*}\det\left(M\right) - 1}{M_{11} + k_{11}^{*2}M_{22} - 2k_{11}^{*}} \tag{7}$$

Table 1: Parameters used in the simulation.

Parameters	**Description**	**Value**
n_g	Group velocity	3.6416
λ_0	Center wavelength	1.55 µm
n_{eff0}	Effective refractive index at the center wavelength	2.7136
n_{imo}	Imaginary part of effective refractive index at the center wavelength	1.357e-5
R	Radius of the ring	30 µm
D	Duty cycle of the grating	0.5
N	Number of periods of the grating embedded in the ring	660
Γ	Confinement factor of III-V waveguide	0.1
n	Effective refractive index of III-V	3.2
L	Effective length of the cavity	1500 µm
N_g	Number of periods of the DBR	15
r_{g12}	Reflectivity of the grating	0.045
n_{effs}	Effective refractive index of slot	2.523
n_{effg}	Effective refractive index of ridge	2.838

(1)
(2)
(3)

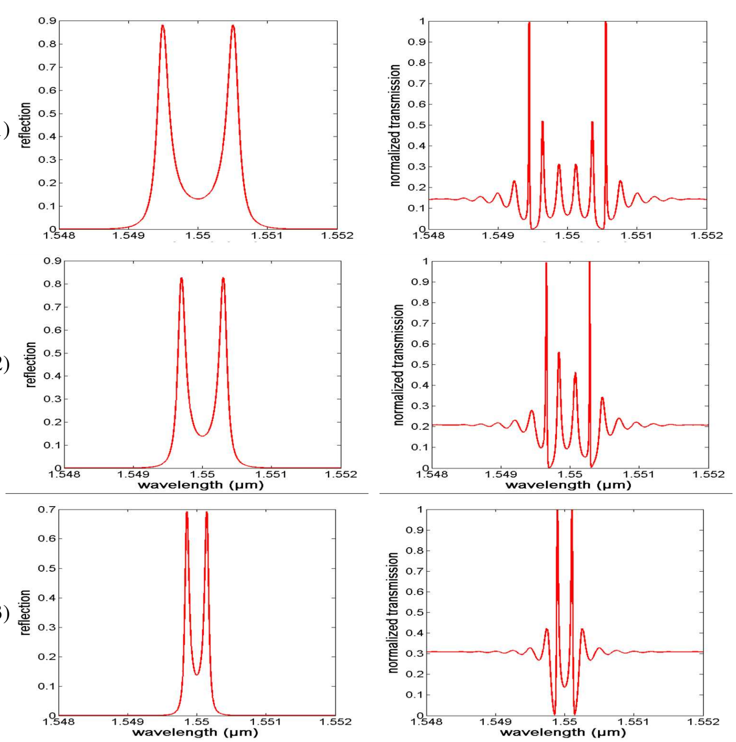

(a) (b)

Figure 4: (a) The reflection spectrum of GMR. (b) The transmission spectrum of whole DWL cavity. (1) When $r = 0.0007$, $k_{11} = 0.85$; (2) when $r = 0.00042$, $k_{11} = 0.9$; (3) when $r = 0.0002$, $k_{11} = 0.95$.

3. SIMULATION RESULTS

The parameters of the DWL used for the simulation are listed in Table 1.

The reflection spectrum of GMR changes with r, as shown in Fig. 3. When the self-coefficient is settled, the coupling between the two counter-propagating modes becomes stronger with the increase of reflection coefficient r, so the splitting appears.

Adjusting the phase section together with GMR parameters, we can obtain two lasing peaks at two wavelengths of different intervals, as shown in Fig. 4. The difference between the two lasing wavelengths are 1.0 nm, 0.6 nm, 0.2 nm, respectively. It is shown that r will decide the gap between the two lasing peaks. When the gap becomes narrower, k_{11} need to be increased to get a larger side mode suppression ratio.

4. CONCLUSION

We demonstrate a novel design of a DWL, which is based on the reflection spectrum splitting in a grating embedded ring. By varying the ring coupling coefficient and grating reflectivity, we can change the interval between two lasing wavelengths from 0 to 1 nm.

ACKNOWLEDGMENT

This work was supported by the National High-Tech R&D Program of China (grant No. 2013AA014401), and the National Natural Science Foundation of China (grant No. 61377038).

REFERENCES

1. Federici, J. and L. Moeller, "Review of terahertz and subterahertz wireless communications," *Journal of Applied Physics*, Vol. 107, No. 11, 111101, 2010.
2. Grosskopf, G., et al., "Optical millimeter-wave generation and wireless data transmission using a dual-mode laser," *IEEE Photonics Technology Letters*, Vol. 12, No. 12, 1692–1694, 2000.
3. Mao, W., et al., "All-optical clock recovery from RZ-format data by using a two-section gain-coupled DFB laser," *Journal of lightwave technology*, Vol. 20, No. 9, 1705, 2002.
4. Schneider, G. J., et al., "Radiofrequency signal-generation system with over seven octaves of continuous tuning," *Nature Photonics*, Vol. 7, No. 2, 118–122, 2013.
5. Kim, N., et al., "Monolithic dual-mode distributed feedback semiconductor laser for tunable continuous-wave terahertz generation." *Optics Express*, Vol. 17, No. 16, 13851–13859, 2009.
6. Lo, Y.-H., et al., "Tunable microwave generation of a monolithic dual-wavelength distributed feedback laser," *Optics Express*, Vol. 22, No. 11, 13125–13137, 2014.
7. Carpintero, G., et al., "95 GHz millimeter wave signal generation using an arrayed waveguide grating dual wavelength semiconductor laser," *Optics Letters*, Vol. 37, No. 17, 3657–3659, 2012.
8. Klehr, A., et al., "High-power monolithic two-mode DFB laser diodes for the generation of THz radiation," *Selected Topics in Quantum Electronics, IEEE Journal of*, Vol. 14, No. 2, 289–294, 2008.
9. Shao, H., et al., "Heterogeneously integrated III–V/silicon dual-mode distributed feedback laser array for terahertz generation," *Optics Letters*, Vol. 39, No. 22, 6403–6406, 2014.
10. Huang, Q., et al., "Ultracompact Adiabatic Tapered Coupler for the Si/III-V Heterogeneous Integration," *PIERS Proceedings*, 2014.
11. Kang, Y. M., A. Arbabi, and L. L. Goddard, "Engineering the spectral reflectance of microring resonators with integrated reflective elements," *Optics Express*, Vol. 18, No. 16, 16813–16825, 2010.